



Research Article

Theme: Celebrating Women in the Pharmaceutical Sciences

Guest Editors: Diane Burgess, Marilyn Morris and Meena Subramanyam

Elucidating the Effect of Fine Lactose Ratio on the Rheological Properties and Aerodynamic Behavior of Dry Powder for Inhalation

Ying Sun,¹ Lu Qin,¹ Jiayi Li,¹ Jian Su,¹ Ruxiao Song,¹ Xin Zhang,¹ Jian Guan,¹ and Shirui Mao^{1,2}

Received 4 January 2021; accepted 15 March 2021; published online 15 April 2021

Abstract. Dry powder inhaler (DPI) is recognized as the first choice for lung diseases' treatment. However, it lacks a universal way for DPI formulation development. Fine lactose is commonly added in DPIs to improve delivery performance; however, the fine ratio-dependent mechanism is unclear. Therefore, the objective of this study is to explore the influence of fine lactose ratio on DPI powder properties and aerodynamic behavior, and the fine lactose ratio-dependent mechanism involved during powder fluidization and lung deposition. Here salbutamol sulfate was used as a model drug, Lactohale® 206 as coarse carrier, and Lactohale® 300 as fine component; the mixtures were prepared at 1% drug content, with fine content up to 20%. It was shown that with the fine addition, flowability of the mixtures was improved, interaction among particles was increased, and the presence of fines could help to improve DPI's aerosolization performance. When the fines added were less than 3%, the "active site" hypothesis played a leading role. When the added fines were over 3% but less than 10%, fluidization enhancement mechanism was more important. After the added fines reaching 10%, aggregate mechanism started to dominate. However, FPF cannot be further increased once the fines reached 20%. Moreover, the correlations between FPF and dynamic powder parameters were verified in ternary mixtures, and cohesion had a greater impact on FPF than that of flowability. In conclusion, adding lactose fines is an effective way to improve lung deposition of DPI, with the concrete mechanism lactose fine ratio dependent.

KEY WORDS: dry powder inhaler (DPI); fine lactose ratio; fines mechanism; lung deposition prediction.

INTRODUCTION

In recent years, lung-related diseases are increasing rapidly, and drug delivered directly to the lung is the recommended route for pulmonary diseases therapy because

of its superior advantages (1), such as direct target to the lung with low dose and side effects. Especially, dry powder inhaler (DPI) is attracting more attention based on good stability and ease of coordination. However, drug dispersion performance (fine particle fraction, FPF) of currently available DPIs is only in the range of 20–30% even at 30 L/min inspiratory air flow or higher (2), which is controlled by the balance between drug particles/carrier interaction and air separation force. The DPI inhalation process involves a number of complex steps (3), such as powder fluidization, deagglomeration, dispersion and transportation through the airways, and finally deposition. Thus, DPI products with appropriate flowability and cohesion are desired for better lung deposition; however, the balance needs to be well controlled.

In general, in order to obtain a favorable performance, the micronized active drugs are commonly mixed with coarse carrier particles to increase the flowability(4). Thus, most DPI products are physical mixtures of micronized drugs with lactose as carriers. However, detaching the micronized drug from carrier particles might be a challenge during powder fluidization and aerosol formation. Therefore, in order to tailor the aerosolization behaviors of DPI powders, some

¹ School of Pharmacy, Shenyang Pharmaceutical University, 103 Wenhua Road, Shenyang, 110016, China.

² To whom correspondence should be addressed. (e-mail: maoshirui@syphu.edu.cn; maoshirui@vip.sina.com)

Abbreviations: DPI, Dry powder inhaler; FPF, Fine particle fraction; MFV, Minimum fluidization velocity; SS, Salbutamol sulfate; LH206, Lactohale® 206; LH300, Lactohale® 300; RH, Relative humidity; RSD, Relative standard deviation; PSD, Particle size distribution; SEM, Scanning electron microscopy; BFE, Basic flowability energy; AEnorm, Normalized aeration energy; AR, Aeration ratio; PD, Pressure drop; FF, Flowability function; NGI, Next Generation Impactor; HPLC, High-performance liquid chromatography; EF, Emitted fraction; MMAD, Mass median aerodynamic diameter; SD, Standard deviation; D10, Volumetric diameter value at 10% of cumulative distribution; D50, Volumetric diameter value at 50% of cumulative distribution; D90, Volumetric diameter value at 90% of cumulative distribution; PCA, Principal component analysis; PC(1,2), Principal component(1,2); TCS, Total component score.

additives such as lactose fines (5), magnesium stearate (6), or leucine(6, 7) are added in the mixture to serve as deagglomeration facilitators with improved flowability and decreased cohesion. Numerous studies have revealed that the presence of additives enhanced powder aerosolization performance based on several theories. “Active site” (8, 9) theory suggests that fine powders would preferentially occupy the strong binding sites at the carrier surface; then, drug particles occupy the other sites with weaker binding force. As for agglomeration theory, it describes that some aggregates composed of drug particles and fine powders can be formed during the mixing process, which increases the distance between drug particles and carriers, thus reducing the force among them. Moreover, compared with single drug particles, drug aggregates have greater inertial force and aerodynamic drag force to disperse (10, 11). Fluidization enhancement mechanism is correlated with the increased minimum fluidization velocity (MFV) of powder in presence of fines, improving particles colliding energy with each other(12). Buffer mechanism assumes the fines will protect the drug particles from suffering the mixing pressure generated during collision with carriers (13). Fine particle network mechanism supposes that fines with a slightly larger particle size can improve drug dispersion performance by preventing the network structure formation on carrier surface (14, 15). All the above five hypotheses can play a positive role in enhancing aerodynamic behavior of DPI powders; however, a negative influence might be caused by the press-on mechanism(14), which indicates that a stronger inertial and frictional forces (press-on forces) can exert on DPI powders during mixing with fines, making drugs adhere firmly to the carrier surface, and unable to detach at flow rates < 40 L/min.

Based on the description above, the added fines can affect DPI performance by influencing the molecular interaction between drug and carrier, powder properties (particle size, surface properties, fluidization, and deagglomeration), and thus drug detachment during inhalation, therefore varied lung deposition delivery efficiency. However, the content of fine lactose on the rheological properties and aerodynamic behavior of DPIs, as well as fine lactose ratio-related mechanisms involved, has not been systematically studied, and no enough experimental data are available to provide favorable support to the above hypotheses. Moreover, it is known that flowability and interparticulate interaction (such as powder cohesion) of DPI formulations could affect their fluidization and deagglomeration behavior, and finally the aerosolization performance. However, these fundamental powder mechanics and their critical relation with delivery process remain poorly understood. Therefore, further investigation is required to clarify the correlation between DPI powder bulk behavior and aerosol performance for potential lung deposition prediction.

Thus, the objective of this study is to explore the influence of fine lactose ratio on DPI powder rheological properties and aerodynamic behavior, and elucidate the main mechanism involved for the improved aerodynamic performance at specific fine ratios. Moreover, this study also tries to connect powder rheological properties with DPI inhalation process, to investigate the feasibility of predicting *in vitro* lung deposition of ternary DPI formulations.

MATERIALS AND METHODS

Materials

Salbutamol sulphate (SS) as model drug was from Shandong Xiya Reagent Pharmaceutical Ltd (China). Lactohale® 206 as coarse carrier (hereafter called LH206) and Lactohale® 300 as fine lactose (hereafter called LH300) were supplied by DFE Pharma (China). All other reagent was of analytical grade and used as received, unless otherwise specified.

Preparation and Characterization of DPI Formulations

DPI formulations were prepared and characterized as reported previously (16, 17). Briefly, SS was firstly milled by Jet mill lab (Noozle Technology, China) at 6.5 bar pressure to obtain an inhalable size. Then, drug particles, carriers, and fines were sieved through a 425- μ m sieve to break up large aggregates and conditioned at 20 ± 2 °C and $45 \pm 5\%$ RH for 24h (18). Thereafter, specific ratios of fines and carriers were handled via a manual geometric mixing; then, the drug was added to such pre-mixtures, followed by an intensive mixing at 100 rpm for 5 min and 300 rpm for another 4 min with Mini-G Wet mixer (Xin Yi Te Technology Co., Ltd. China). One hundred eighty grams of physical mixtures with different fine contents of 1%, 3%, 5%, 7%, 10%, 15%, and 20% (w/w) was prepared respectively.

Recovery rate was calculated using the following Eq. (1), drug content was analyzed by a UV spectroscopy method (Unico, Shanghai). RSD (relative standard deviation, %) of the recovery rate was used to represent blend uniformity.

Recovery rate

$$= (\text{measured drug content}/\text{theoretical drug content}) \times 100\% \quad (1)$$

Particle size distribution (PSD) of the materials was determined using a Sympatec HELOS/KP laser diffraction equipment (Sympatec GmbH, Clausthal-Zellerfeld, Germany) with the RODOS dry dispersion mode, and 4 bar pressure was used to efficiently disperse the particle agglomerates. R1 measurement lens was used for drugs and fines, and R5 lens for mixtures and carriers. Measurements were repeated in triplicate.

Morphology Characterization

Morphology was characterized with scanning electron microscopy (SEM). Mixtures (ca. 20 mg) were sprinkled gently on aluminum specimen connected with carbon sticker, and then, excess specimens were removed. The powders were finally coated with gold to prevent charging effect, and visualized with Hitachi S-3400 (Hitachi, Tokyo, Japan).

Surface Area Measurement

Surface area of the fines and carriers was measured by BET nitrogen adsorption method with a Surface Area Analyzer (ASAP 2460, Micromeritics, UK). Briefly, before analysis, the samples (ca. 0.5 g) were placed at 75. Bin a glass holder for 10 h to degas. BET surface area was recorded as the specific surface area with nitrogen as adsorbate. And then, surface coverage ratio (SCR) was calculated to reflect the relationship between surface area of the carrier and projected area of the fines adhered to the carrier surface, according to the following Eq. (2) as reported previously (19).

$$SCR = (\alpha \cdot m_f \cdot S_{w,f}) / (m_c \cdot S_{w,c}) \quad (2)$$

where m_f and m_c are the mass of fines and carrier particles in the mixture and $S_{w,f}$ and $S_{w,c}$ are the specific surface area of the fines and carrier particles. The factor α can be set equal to $1/\pi$ based on the assumption that a rectangular packing, while the fines or carrier particles are not completely spherical.

Powder Rheological Properties' Measurement

Powder rheological properties were characterized with a FT4 rheometer (Freeman Technology, UK) according to the method reported previously (16, 17).

In dynamic measurement mode, filled the test powders (ca. 20 g) into the customized vessel (25 mm*25 mL), then recorded the data of rotational torque, axial force, and displacement for calculating the flow energy required during powder displacement, and defined it as basic flowability energy (BFE). Took another powders (ca. 18 g) and put them in another vessel (25 mm*35 mL), from the bottom introduced a range of airflow (0, 2, 4, 6, 8, and 10 mm/s) successively. Once the powder was fluidized completely, the flow energy required would remain constant, and defined it as aeration energy (AE) or fluidization energy. Moreover, another parameter related with AE, aeration ratio (AR), was defined as shown in Eq. (3).

$$AR = (\text{Energy at 0 mm/s of air flow rate (BFE)}) / (\text{aeration energy (AE)}) \quad (3)$$

In bulk measurement mode, placed powder (ca. 9 g) into the customized vessel (25 mm*10 mL) with 2 mm/s airflow introduced. Permeability was measured with the obtained pressure drop (PD) at 15 kPa normal stress and calculated with Darcy's law (20).

In shear cell measurement mode, the powder (ca. 9 g) was also placed into the customized vessel (25 mm*10 mL) with a series of pre-defined vertical stress to the powder bed to draw a Mohr circle, and then, the related flowability function (FF) and cohesion were obtained.

Aerodynamic Properties' Characterization

Aerodynamic properties of DPI powder were measured using a Next Generation Impactor (NGI, Copley Scientific,

UK) and performed at 100 L/min for 2.4s with Cyclohaler® device (Teva Pharmaceuticals, The Netherlands) (16, 17). Prior to measurement, all the impactor stages and pre-separator were pre-coated with 10% (w/v) Tween-20 ethanol solution. Filled 25 mg mixture into Vcaps® (No. 3 HPMC capsule, Capsugel®, China), and 7 capsules were used in one run. After operation, deposited drug particles were collected with distilled water and drug content was analyzed by high-performance liquid chromatography (HPLC, Agilent Technologies, Inc) method. Three aerodynamic performance-related parameters, including emitted fraction (EF), fine particle fraction (FPF), and mass median aerodynamic diameter (MMAD), were also determined. EF is the ratio of drug emitted from inhaler device (collected from artificial throat, pre-separator, and all stages of impactor) to the recovered dose (collected from capsules, device, artificial throat, pre-separator, and all impactor stages). FPF is the mass percentage of drug with an aerodynamic diameter in the range of 0.5–5 μm , calculated as the ratio of drug deposited at stages 1–5 to the recovered dose. All NGI experiments were performed in triplicate.

Drug Content Analysis by HPLC

Deposited salbutamol sulfate content in the NGI test was quantified using the HPLC method described in Chinese Pharmacopoeia. Briefly, Amethyst C18-H (150 mm \times 4.60 mm, 5 μm) chromatographic column was used. The mobile phase was composed of buffering system (85%) (containing 11.04 g/L NaH_2PO_4 aqueous solution [$\text{NaH}_2\text{PO}_4 \cdot 2\text{H}_2\text{O}$ 12.4808 g, 1000 mL of distilled water was added, pH was adjusted to 3.10 ± 0.05 with 85% H_3PO_4]) and methanol (15%). The flow rate was set at 1.0 mL/min and the UV detection wavelength was 276 nm.

Statistical Analysis

Experimental values were expressed as mean \pm standard deviation (SD) from at least three measurements unless otherwise specified. Two-tailed *t*-test comparison was used for statistical analysis, with probability values $p < 0.05$ considered as statistically significant.

RESULTS AND DISCUSSION

Influence of Fine Lactose Ratio on Particle Size and Uniformity of the Mixture

In this study, using salbutamol sulfate (SS) as a model drug, LH206 as coarse lactose carrier, and LH300 as fine lactose, their physical mixture was prepared at 1% drug content and fine lactose content was within 20%. It is anticipated that the added fines can change carrier surface, as well as the interaction between drug particles and carriers, therefore properties of the DPI powders.

As shown in Table I, SS is in an inhalable size range of 0.5–5 μm . LH206 has an average particle size of about 80 μm , which is sufficient to ensure dose accuracy and uniformity (21). Moreover, the very limited fines existed in LH206 can also prevent interference of the external fines added. The size of added fines LH300 ($D_{50} = 2.86 \pm 0.02 \mu\text{m}$) is larger than

that of the micronized drug, but significantly smaller than that of the lactose carrier. It was noted that the added fines had remarkable influence on the mixtures' size. When the added fines were less than 10%, D10, D50, and D90 of the ternary physical mixtures were significantly smaller than those of LH206 ($p < 0.05$). However, when the fines reach 15%, D90 of the mixture was larger than that of LH206, implying the micronized drug or lactose fines might rearrange and redisperse on the surface of the carrier (12, 22). At this stage, a large fine-fine aggregates or drug-fine aggregates might be formed in the mixture, and D90 is sensitive to such change of larger particle size components; therefore, D90 started to increase when the fines exceeded 10%.

Morphology observation further confirmed the particle size results presented in Fig. 1. Lactose carrier LH206 was tomahawk-shaped with some sunk parts on the surface; when the fine ratio was no more than 3 wt%, they predominantly filled in such sunk parts of the carrier. With fines continued to increase, they attached to the carrier's outer surface and became an adhesion layer (≤ 10 wt%). At a higher fine concentration (15–20 wt%), a second phase composed of fines was formed. As shown in Table II, surface coverage ratio (SCR) was lactose fine ratio dependent, and it reached over 50% at lactose fine content of 15%. Thus, part of the added LH300 failed to adhere to the carrier surface, forming larger agglomerates, which might cause segregation.

In addition to particle size, span value was used to describe particle size distribution, it was found (Table I) that the mixtures' span value became larger with the fines increase when compared with LH206 ($p < 0.05$). This is quite reasonable while the fines added could increase the proportion of small particle size components in the mixture, and increase of the span value was more apparent when fine aggregates were formed in the system (fines $> 10\%$). Good blend uniformity (represented by RSD in Table I) was observed when LH300 ratio was less than 10%, and it increased thereafter; this is also in agreement with the particle size change and morphology of the physical mixtures observed in Fig. 1, attributed to drug-fine or fine-fine aggregates' formation at this stage. Moreover, the recovery rate and blend uniformity of such mixtures were further investigated after 6-month storage (20 ± 2 °C and $45 \pm 5\%$ RH); it was found that drug recovery rate decreased slightly when the fines exceeded 10% in the mixtures, probably the higher surface energy of fine lactose caused part of the drug-fine powder aggregates adhering to the wall of the storage bottle, resulting in drug loss. However, a 6-month storage did not have a significant impact on RSD, implying no obvious drug segregation during storage (Table I).

Influence of Fine Lactose Ratio on Powder Rheological Properties of the Mixtures

Our previous studies indicated that flowability and cohesion could affect DPI's fluidization, dispersion, and disaggregation behavior when being delivered from the device (16, 17), and such behaviors are crucial for lung deposition efficiency of powders. Therefore, first of all, influence of fine lactose ratio on DPI powder rheological properties, including powder flowability and cohesion, was investigated.

Here, BFE was used to describe powder flowability; in general, a smaller BFE value is correlated with better flowability (23) and it is recognized as a parameter dominating drug release from the capsule and device and further delivery. As shown in Table III, BFE decreased with LH300 content increase ($x \leq 20\%$) in almost a linear manner ($BFE = -11.418x + 339.85$, $R^2 = 0.90$, $n = 8$), implying flowability of the mixtures was improved with fines' addition. Such phenomenon can be attributed to the fines' lubricating effect (19, 20), that is, the added fines covered on the carrier surface can reduce the mechanical gaps among the coarse particles, thereby reducing the resistance during powder flow, leading to improved flowability of the whole mixture.

Influence of fine lactose ratio on cohesion of the mixtures was further investigated. On the one hand, the micronized API should have suitable interaction with carrier particles to ensure stability of the DPI powder during storage, transportation, and delivery (24). On the other hand, drug particles should be able to separate from carriers easily under the appropriate airflow to ensure sufficient deagglomeration. Therefore, the interaction between API and carrier particles should be well balanced. Here, a variety of interaction parameters are used to characterize the dynamic change of API-carrier interaction with the addition of different fine ratios, including AEnorm, AR, Permeability, and molar circle derived parameters, such as Cohesion and FF.

AEnorm is the energy required for complete fluidizing a unit mass of powder in unconstrained measurement when airflow being introduced; in general, a larger AEnorm value is correlated with a greater cohesion of the mixture (23). As shown in Table III, initially, AEnorm increased with LH300 ratio increase ($x \leq 7\%$) ($AEnorm = 0.275x + 1.237$, $R^2 = 0.77$, $n = 5$) and it reached maximum at 7% fine content; thereafter, AEnorm showed a downward trend with further increase of fines, implying the highest cohesion was achieved at lactose fine ratio 7%. Probably when the fines added were less than 7%, they can fill the cracks (also named as "active sites") on carrier surface and then gradually distributed on the carrier surface to form a smooth adhesion layer. At this stage, under the airflow, the fine lactose and the carrier lactose could fluidize as a whole (20, 25). Therefore, the more fines added, the greater the fluidization resistance, as reflected by AEnorm increase. However, when the fines reached 10%, fine aggregates with loose structure began to form in the mixture system, and their fluidization resistance was much smaller compared with the mechanical inlay of fine lactose and carrier lactose; therefore, AEnorm decreased gradually. In addition, AR, a derivative parameter from AE, was also characterized. As a general rule, a larger AR value is correlated to increased sensitivity to air thus easier to fluidize (26). It was noted that AR showed a downward trend ($AR = 17.682e^{-0.162x}$, $R^2 = 0.78$, $n = 6$) with the increase of LH300 ($x \leq 10\%$), implying the fluidization difficulty increased with the addition of lactose fines and reached maximum at lactose fine 10%.

In addition, permeability and molar circle-derived parameters (cohesion and FF), which are more related to cohesion of the powder at a constrained state, were also characterized. The permeability decreased exponentially with the increase of lactose fines (Permeability = $25.315E$

Table I. Particle Size and Uniformity of the Mixtures (*n* = 3)

Material	D10 (µm)	D50 (µm)	D90 (µm)	Span	Particles < 5 µm (%)	Recovery rate (%)	RSD (%)	6-month recovery rate (%)	6-month R S D (%)
SS	0.58 ± 0.03	1.97 ± 0.04	5.03 ± 0.10	2.26 ± 0.08	89.92 ± 0.54	–	–	–	–
LH206	28.43 ± 0.45	79.59 ± 0.65	156.22 ± 0.07	1.61 ± 0.02	2.56 ± 0.10	–	–	–	–
LH300	0.61 ± 0.01	2.86 ± 0.02	7.39 ± 0.22	2.37 ± 0.06	75.44 ± 0.61	–	–	–	–
99%LH206-1%SS	24.56 ± 0.74*	78.15 ± 0.73	153.86 ± 1.58	1.65 ± 0.04	3.82 ± 0.15*	92.68 ± 1.96	± 2.12	93.13 ± 1.86	± 2.00
1% LH300-98%LH206-1%SS	20.54 ± 0.64*	76.49 ± 0.31*	154.92 ± 0.26*	1.76 ± 0.02*	4.88 ± 0.24*	92.68 ± 1.59	± 1.71	93.01 ± 0.92	± 0.99
3% LH300-96%LH206-1%SS	10.62 ± 0.10*	74.75 ± 0.12*	154.45 ± 1.15	1.92 ± 0.02*	7.06 ± 0.05*	95.58 ± 3.54	± 3.71	92.68 ± 1.21	± 1.30
5% LH300-94%LH206-1%SS	5.88 ± 0.03*	71.84 ± 0.27*	152.95 ± 1.55*	1.81 ± 0.03*	9.61 ± 0.03*	94.35 ± 2.23	± 2.36	94.80 ± 2.37	± 2.50
7% LH300-92%LH206-1%SS	4.42 ± 0.05*	70.31 ± 0.64*	151.23 ± 0.75*	2.09 ± 0.02*	11.74 ± 0.16*	94.24 ± 1.18	± 1.25	92.79 ± 0.22	± 0.24
10%LH300-89%LH206-1%SS	3.56 ± 0.02*	66.81 ± 0.40*	152.49 ± 1.77*	2.23 ± 0.02*	15.02 ± 0.09*	95.69 ± 2.23	± 2.33	92.34 ± 1.48	± 1.60
15%LH300-84%LH206-1%SS	2.97 ± 0.01*	62.05 ± 0.11*	159.47 ± 2.52	2.52 ± 0.04*	18.86 ± 0.07*	93.01 ± 5.90	± 6.35	90.78 ± 3.10	± 3.42
20%LH300-79%LH206-1%SS	2.50 ± 0.07*	54.61 ± 2.84*	164.61 ± 3.65*	2.97 ± 0.09*	23.52 ± 0.78*	90.67 ± 5.49	± 6.05	88.88 ± 1.18	± 1.33

**p* < 0.05, compared to LH206 group
 SS, salbutamol sulfate; LH206, Lactohale® 206; LH300, Lactohale® 300

$-0.094x$, $R^2 = 0.96$, $n = 8$), whereas the cohesion, which represents inter-particle force (including the sum of van der Waals force, capillary, and electrostatic force (27)), increased linearly (Cohesion = $0.068x + 0.358$, $R^2 = 0.98$, $n = 8$), with almost linear decrease of FF value ($FF = -0.388x + 9.239$, $R^2 = 0.86$, $n=8$) with the fines' ratio increase ($x \leq 20\%$). These results are quite reasonable while the added fines could occupy the pores of the carrier surface, therefore increasing

the resistance of air flow through the powder, leading to air permeability decrease and cohesion increase. In general, when the FF value was lower than 4, the powder will be difficult to flow (28). It was noted this is the case when the lactose fines reached 15%. Thus, taking both flowability and cohesion into consideration, the content of fine lactose should be kept less than 10%; this needs to be further confirmed via lung deposition study.

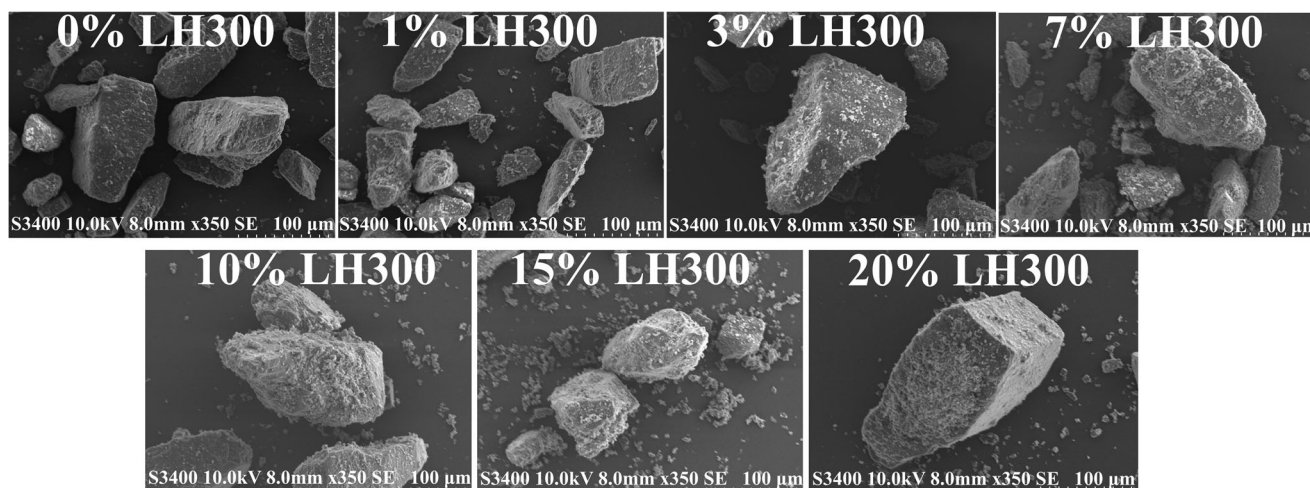


Fig. 1. Morphology of the physical mixtures (1% SS+ LH206+LH300) visualized with SEM. Images taken at × 350 magnification

Table II. Surface Coverage Ratio of the Lactose Mixtures (LH206+LH300) Without 1% SS

Material	Surface area (m ² /g)	Surface coverage ratio (%)
LH300	3.59 ± 0.13	-
LH206	0.37 ± 0.02	-
1%LH300-98%LH206	-	3.12 ± 0.06
3%LH300-96%LH206	-	9.55 ± 0.18
5%LH300-94%LH206	-	16.26 ± 0.30
7%LH300-92%LH206	-	23.25 ± 0.43
10%LH300-89%LH206	-	34.34 ± 0.63
15%LH300-84%LH206	-	54.57 ± 1.01
20%LH300-79%LH206	-	77.37 ± 1.42

SS, salbutamol sulfate; LH206, Lactohale® 206; LH300, Lactohale® 300

Influence of Fine Lactose Ratio on Aerodynamic Properties of the Mixtures

Influence of lactose fine ratio on aerodynamic properties was further investigated using NGI. As shown in Fig. 2a, with the fine lactose ratio increase up to 15%, drug deposition decrease in capsules and inhalers, induction port, and pre-separators was observed; instead, increased drug deposition was noted at 1–5 collection stages in a fine lactose ratio-dependent manner, proving that the added fine lactose can indeed prevent drug deposition in early delivery stages, such as in oropharynx and large trachea, and simultaneously help drug particles deliver to lower respiratory tract successfully (20). Such behavior was closely related to the state of the mixtures as shown in Fig. 1. When the fine ratio was low, the fines were mainly distributed around the carrier's inner surface, filling its irregular sites. Therefore, it is rather difficult to be released during inhalation, leading to low lung deposition. In contrast, with the increase of fines ratio, an adhesive layer could be formed covering the carrier surface, and the interaction among particles in the mixture would also increase as reflected by the increased cohesion value (Table I). Once the carrier surface was fully occupied by the fine lactose, as in the case when the fine ratio was over 10%, they might self-aggregate to form more stable drug-fine

aggregates, separated from the carrier as a second phase and existed alone. This explained the plateau phenomenon observed in 15% and 20% fine mixtures. Therefore, aerodynamic behavior of the mixture was dependent on the existing state of the added fines in the system.

Moreover, three parameters, EF, FPF, and MMAD, were selected to further analyze the influence of fine ratio on DPI's aerodynamic performance quantitatively. As shown in Fig. 2b, EF increased slightly ($EF = 0.607x + 80.417$, $R^2 = 0.96$) with LH300 ratio increase up to 15% based on 21 individual values, and an equilibrium was observed thereafter. Similar to that of EF, the FPF value also increased linearly with the increase of LH300 ratio but more rapidly up to 15% fine ratio ($FPF = 2.332x + 32.73$, $R^2 = 0.95$).

The above studies demonstrated that the presence of fines could help to improve DPI's dispersion and aerosolization performance in a fine ratio-dependent manner. To further analyze the function and mechanism of the fines at different content ratios, MMAD value of the mixtures was also characterized. When compared with micronized drugs ($D_{50} = 1.97 \pm 0.04 \mu\text{m}$), the MMAD of both binary and ternary mixtures increased significantly ($p < 0.05$) (Fig. 2b), suggesting the API was dispersed in the form of aggregates but to a different extent.

Figure 3 schematically describes the distribution of lactose fines within the mixture system and its tunability on fluidization. When the fine lactose ratio was less than 3%, "active site" mechanism (9) played a major role; this is also well supported by the SEM images of the mixtures (Fig. 1), the low surface coverage (< 10% in Table II), and slight change of the MMAD value (Fig. 2) at fine ratio < 3%. The fines would preferentially occupy pittings on the rough carrier surface when they are premixed with coarse carrier, further preventing drug particles from binding such high energy sites; therefore, the drug can be separated easily from the carrier to increase FPF value.

Once the fines reached or exceeded 3%, the "active site" on the carrier surface tended to be saturated; then, the fluidization enhancement mechanism and aggregation mechanism started to play a role. When the content of added fines was less than 10%, the fluidization enhancement mechanism was more crucial, with the fines gradually covering the carrier surface as characterized by the SEM images (Fig. 1), rapid increase of surface coverage ratio (Table II), and apparent

Table III. Powder Rheological Properties of the Mixtures ($n = 3$)

Material	BFE (mJ)	AEnorm (mJ)	AR	Permeability (10^{-9} cm^2)	FF	Cohesion (kPa)
99%LH206-1%SS	375.33 ± 7.09	0.69 ± 0.11	30.53 ± 5.54	29.55 ± 0.33	11.1 ± 0.20	0.374 ± 0.008
1%LH300-98%LH206-1%SS	349.00 ± 6.00 [#]	1.79 ± 0.25 [#]	11.44 ± 2.00 [#]	25.61 ± 0.53 [#]	9.51 ± 0.60 [#]	0.443 ± 0.028 [#]
3%LH300-96%LH206-1%SS	302.33 ± 8.08 [#]	2.58 ± 0.16 [#]	7.77 ± 0.67 [#]	19.17 ± 0.03 [#]	7.10 ± 0.23 [#]	0.612 ± 0.026 [#]
5%LH300-94%LH206-1%SS	257.67 ± 6.11 [#]	2.65 ± 0.17 [#]	6.84 ± 0.88 [#]	14.62 ± 0.65 [#]	6.46 ± 0.81 [#]	0.677 ± 0.095 [#]
7%LH300-92%LH206-1%SS	234.00 ± 4.58 [#]	2.87 ± 0.26 [#]	5.78 ± 0.42 [#]	11.23 ± 0.20 [#]	5.64 ± 0.29 [#]	0.765 ± 0.045 [#]
10%LH300-89%LH206-1%SS	193.00 ± 3.61 [#]	2.51 ± 0.21 [#]	4.21 ± 0.23 [#]	8.12 ± 0.03 [#]	4.62 ± 0.09 [#]	0.950 ± 0.022 [#]
15%LH300-84%LH206-1%SS	167.67 ± 6.35 [#]	2.27 ± 0.24 [#]	4.77 ± 0.56 [#]	6.11 ± 0.25 [#]	3.10 ± 0.08 [#]	1.487 ± 0.050 [#]
20%LH300-79%LH206-1%SS	143.33 ± 2.52 [#]	1.78 ± 0.08 [#]	3.91 ± 0.21 [#]	4.55 ± 0.02 [#]	2.74 ± 0.09 [#]	1.697 ± 0.058 [#]

[#] $p < 0.05$, compared to 99%LH206-1%SS group

BFE, basic flowability energy; AEnorm, normalized aeration energy; AR, aeration ratio; FF, flowability function; SS, salbutamol sulfate; LH206, Lactohale® 206; LH300, Lactohale® 300

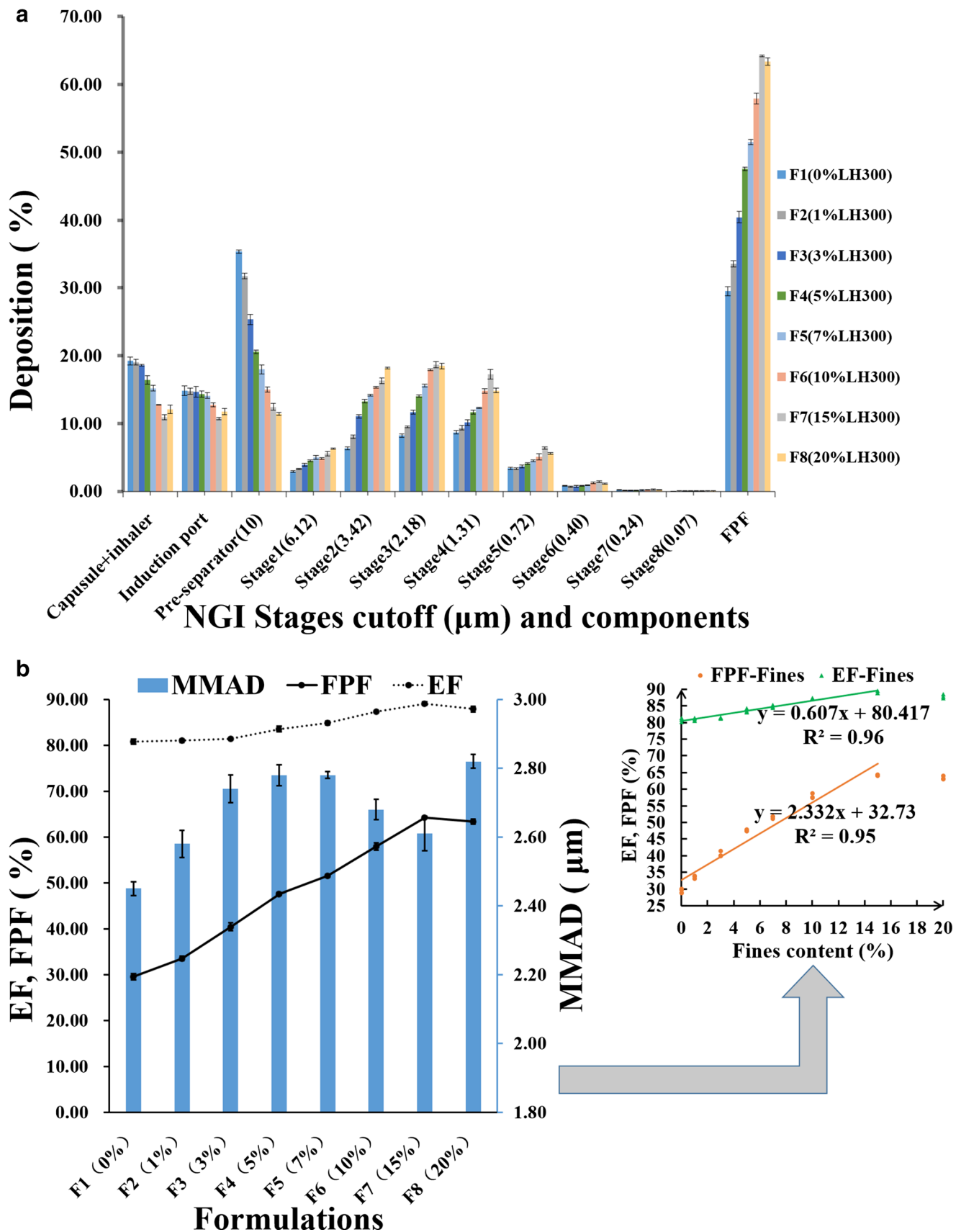


Fig. 2. Aerodynamic properties of all the mixtures characterized by NGI. **a** Aerodynamic particle size distribution. **b** Aerodynamic performance including MMAD, EF, and FPF

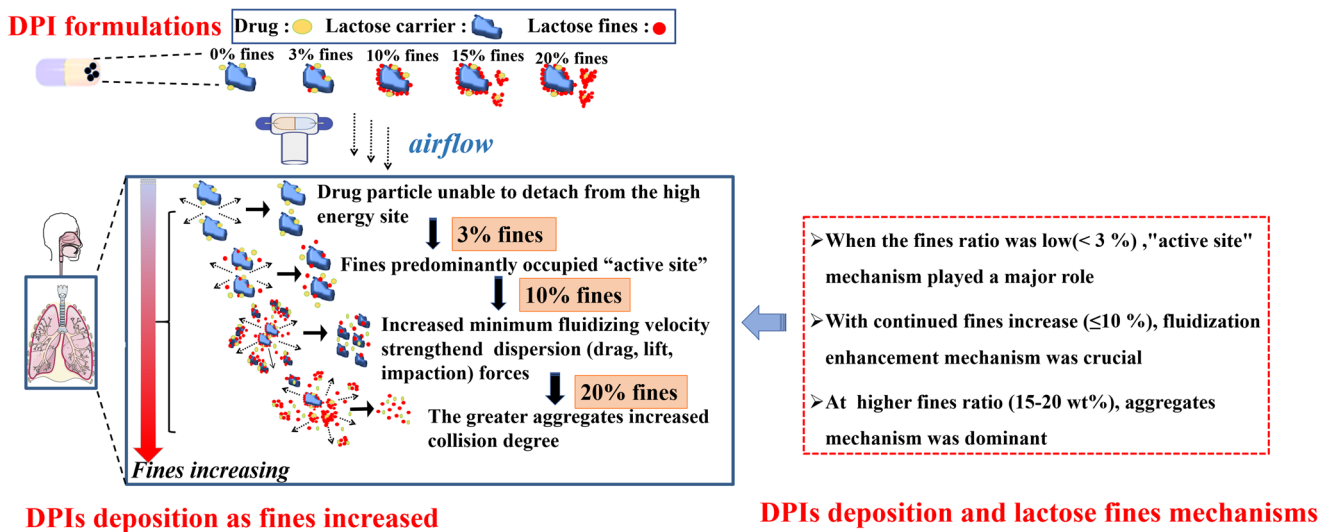


Fig. 3. Interactions of lactose fines within the mixture system and its tunability on DPI deposition

increase in FPF value (Fig. 2). The decreased permeability was related to increased resistance to air flow with the increase of fines (Table I), further improving the minimum fluidizing air flow velocity; therefore, it can strengthen the dispersion force within inhalers during aerosolization (29), leading to an increased FPF. Moreover, the critical points of two parameters AR and FF, which reflected fluidization and flowability/cohesion of the mixture, were also observed at fine ratio 10% (Table I), implying the resistance to air flow changed at this state, suggesting fluidization enhancement

mechanism played a leading role when the ratio of fine lactose was within the first 10%.

However, when the fines added reached 10%, the aggregate mechanism was believed to be dominant. The decreased MMAD value at fine ratio over 10% (Fig. 2b) confirmed the presence of drug aggregates. It was noted that MMAD remained unchanged when the content of fine lactose ratio was in the range of 3–7%. Once the fine content reached 10%, the collision degree among fine aggregates might increase, with large aggregates breaking

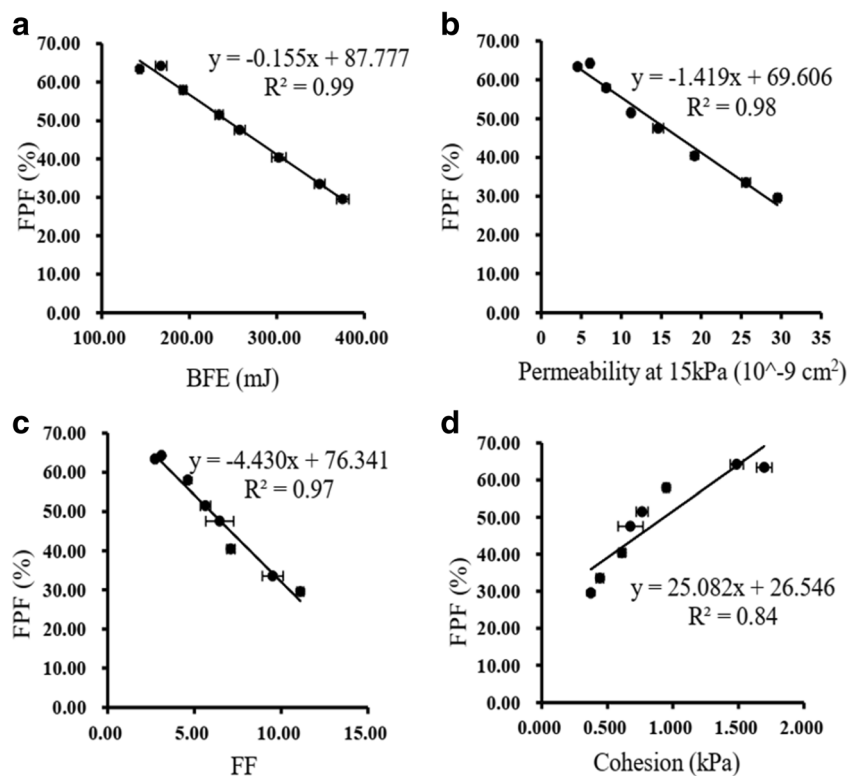


Fig. 4. Correlations between DPI powder properties and FPF of all the mixtures ($n = 3$). **a** BFE-FPF. **b** Permeability-FPF. **c** FF-FPF. **d** Cohesion-FPF

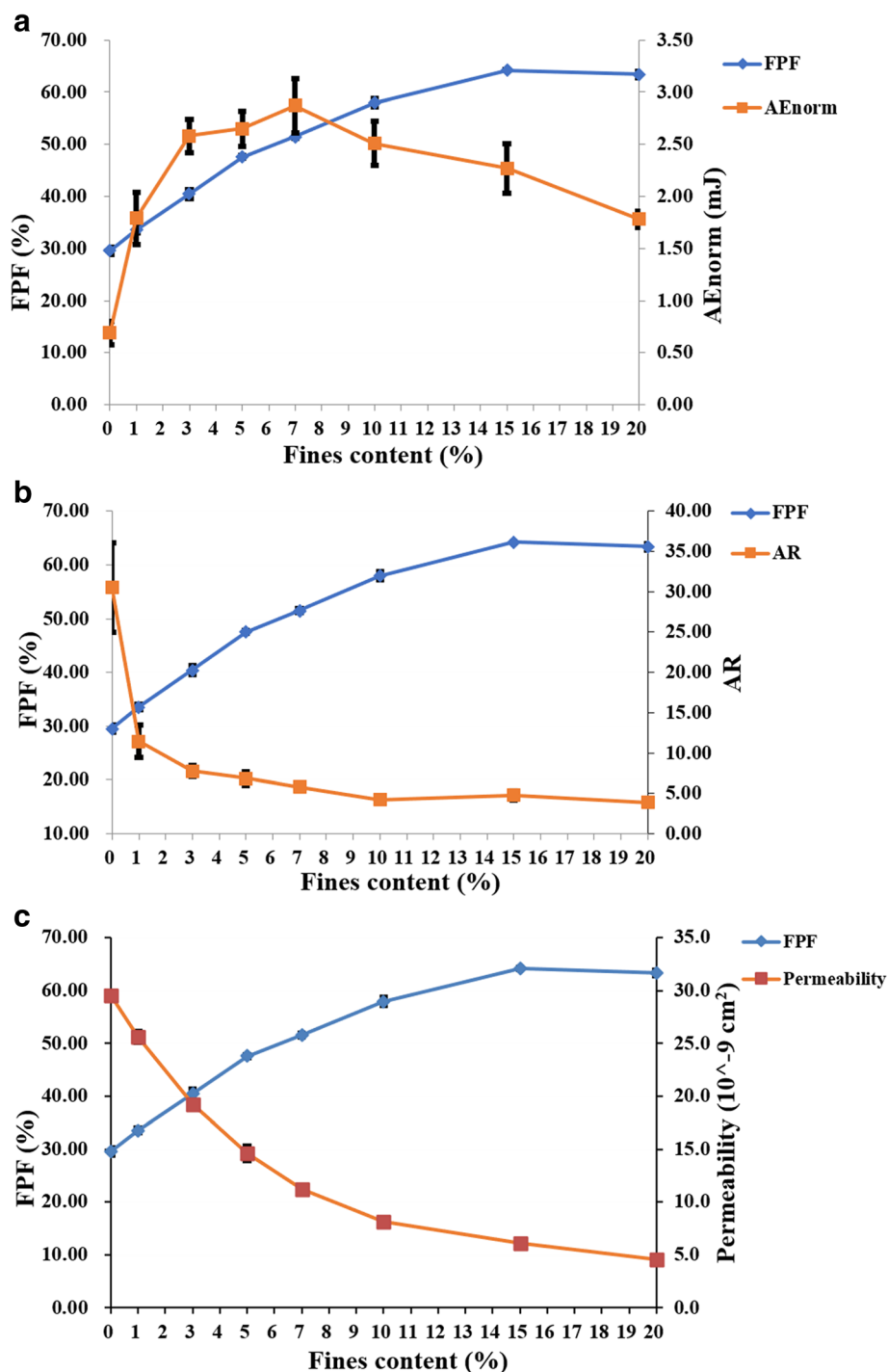


Fig. 5. Effect of lactose fines' ratio on the aerodynamic performance of the DPI powder mixture. **a** FPF and AEnorm. **b** FPF and AR. **c** FPF and Permeability (*n* = 3)

into smaller ones, therefore leading to MMAD decrease. As the content of fines was further increased to 20%, no additional FPF increase was observed, probably the force involved was not sufficient to break more aggregates at this stage. Therefore, we can draw such a conclusion that the aggregates' mechanism was more important when the fines added reached 10%, but fines' addition over 15% is not recommended.

Correlations Between Powder Properties and Lung Drug Deposition Behavior

When drug particles are delivered from DPI device, they must deposit in the lung to take effect. However, small differences in binary or ternary formulation's composition could cause great changes in drug aerosol delivery behavior, which brings great uncertainty for formulation development.

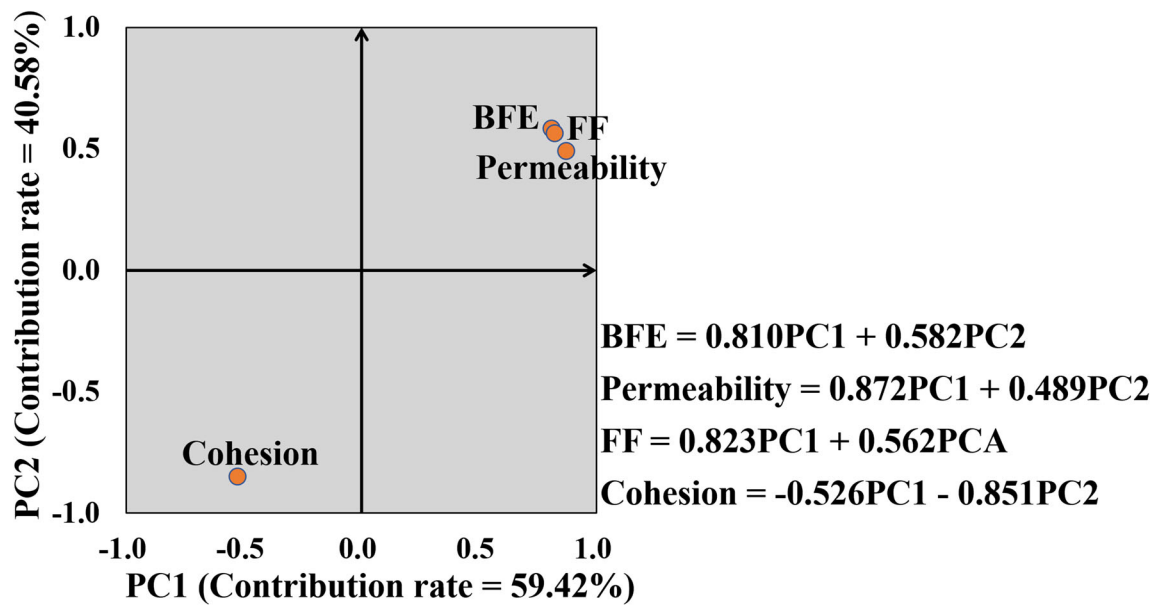


Fig. 6. Component load matrix of rotated principal component matrix from four original powder properties

Therefore, it is highly desirable to establish correlations between DPI powder property-related parameters and downstream deposition performance for better formulation optimization. Here, the correlation between four powder properties, BFE, permeability, FF, cohesion, and FPF value was explored; the results are shown in Fig. 4.

It can be seen from Fig. 4a that BFE was negatively correlated with FPF, that is, a mixture with good flowability is more beneficial for downstream deposition. Generally, drug delivered to the effective site of lung can be divided into four consecutive stages (23): fluidization and dispersion of DPIs, drug transportation, drug detachment from carriers, and drug deposition in lungs. The superior flowability is a precondition for DPIs smoothly released from the inhaler and transported to the respiratory tract. In other words, the better the flowability, the more easily for the drug to deliver into the lung (27). Similarly, negative correlation between permeability and FPF, FF, and FPF was observed (Fig. 4b, c), implying stronger inter-particle interaction is beneficial for drug deposition in the lung. The positive correlation between cohesion and FPF (Fig. 4d) further demonstrated this point. This is in agreement with the above-mentioned aggregation

and fluidization enhancement mechanism, that is, the powders with enhanced cohesion would be lifted as fractures or plugs and then suffered from effective particle-particle and particle-wall collision during aerosolization (12). Furthermore, the increased resistance to air flow (reflected as decreased permeability) also strengthened the dispersion (drag, lift, and impaction) forces within dry powder inhalers (29, 30), leading to a more intense deaggregation behavior, thereby promoting drug detaching from the carrier surface and being successfully deposited in the deep lung, and finally, a satisfactory aerosolization performance was achieved.

Moreover, this study also tried to predict the optimal fines' content via rheological properties. As we can see from Fig. 5a, a parameter representing fluidization difficulty, AEnorm, reached its peak after adding 7% fine lactose. Similarly, AR was at a plateau at fine ratio of 10% and the decrease of permeability slowed down at 10% fines (less than $8 \times 10^{-9} \text{ cm}^2$), suggesting the maximum fluidization energy has been reached and further fines' addition is not recommended. Such inflection point or plateau period of these values was similar to the FPF plateau stage; similar phenomena has been reported previously (20). Therefore, according to the turning point of AEnorm, AR, and Permeability, it can be predicted that the optimal content of fine lactose was about 10% in this study.

Contribution Analysis of Flowability and Cohesion

The results in Fig. 4 indicated both flowability and cohesion properties of the powder mixture can influence its deposition in the lung; however, it is still ambiguous which powder properties could have a greater impact on aerodynamic performance of ternary DPIs and how to balance the flowability and cohesion in DPI formulations. Therefore, in this study, the most representative parameters, BFE, Permeability, FF, and Cohesion, were extracted with principal component analysis (PCA), to endow them practical significance.

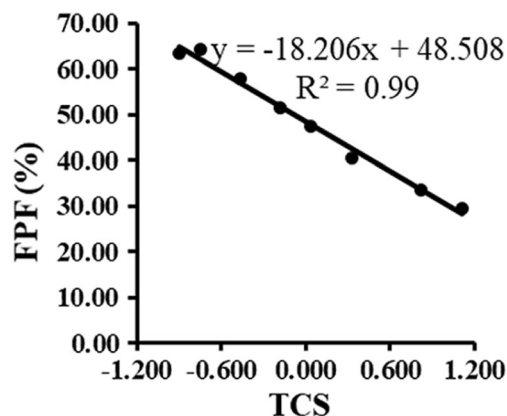


Fig. 7. Correlation between TCS and FPF of all the mixtures

As shown in Fig. 6, two principal components (PCs) can be extracted from the above four powder parameters. And PC1 with 59.42% contribution rate was greater than PC2 (40.58%). Moreover, a good correlation between the original variables and the extracted principal components can be established (Fig. 6); it was noted that the projection of cohesion on PC2 was larger, indicating that cohesion was closely related to PC2. Meanwhile, the projection of BFE, Permeability, and FF on PC1 was larger, confirming BFE, Permeability, and FF were closely related to PC1. Therefore, PC2 can be defined as cohesion index, and PC1 as flowability-cohesion balance index.

Thereafter, the total component score (TCS) was determined according to the contribution rate of both PCs and scores of each component, and as shown in Fig. 7, a good linear negative correlation between TCS and FPF was established, indicating the mixtures should have a lower TCS in order to get a higher FPF value; therefore, the scores of PC1 and PC2 should be lower. To get a lower PC2 value, the cohesion should be large. In contrast, to get a lower PC1 value, the Permeability, BFE, and FF should be low as well. That is, good flowability and strong cohesion are beneficial to improve DPI's aerosolization performance.

It was noted that PC1 was a composite indicator (including BFE, FF, and Permeability) involving both flowability and cohesion; therefore, this study further redistributed the contribution rate of PC1 with the coefficients described at the right of Fig. 6. After BFE being redistributed as flowability index, the other parameters were attributed to cohesion index. The results showed that the contribution rate of cohesion (70.96%) was much greater than that of flowability (29.04%), implying the *in vitro* deposition behavior of DPI was more dependent on cohesion. This is in good agreement with our conclusion drawn from other studies (16).

CONCLUSION

This study explored the influence of fine lactose ratio on DPI powder properties and aerodynamic behavior. Based on the experimental data, the fine lactose ratio-dependent mechanism involved during powder fluidization and lung deposition was explored.

- As the content of fines increased to 20%, flowability of the mixtures was improved, the interaction among particles increased, and the presence of fines also improved DPI's aerosolization performance. It was proved when the added fines were less than 3%, the "active site" hypothesis played a leading role. Once the "active site" over the carrier surface was saturated, both the fluidization enhancement and the aggregate mechanism came into effect. When the added fines were less than 10%, fluidization enhancement mechanism was more important. After the added fines reaching 10%, aggregate mechanism started to dominate. However, FPF cannot be further increased once the fines reach 20%.
- Some correlations between dynamic powder properties and FPF were verified in ternary DPIs, including flowability parameters (BFE) and

interactions parameters (Permeability, FF, and Cohesion). The optimal content of lactose fines can be determined preliminarily according to the evolution of AEnorm, AR, and Permeability. Principal component analysis results showed that cohesion (contribution rate of 70.96%) had a greater impact on FPF than flowability (contribution rate of 29.04%).

FUNDING

This work is financially supported by Chunhui Program of the Ministry of Education of China (2022410012), the National Key R&D Program of China (2020YFE0201700), and the Liaoning Provincial Higher Education Overseas Training Program (2019GJWZD005).

REFERENCES

1. Chennakesavulu S, Mishra A, Sudheer A, Sowmya C, Reddy CS, Bhargav E. Pulmonary delivery of liposomal dry powder inhaler formulation for effective treatment of idiopathic pulmonary fibrosis. *Asian J Pharm Sci.* 2018;13(1):91–100.
2. Yang MY, Chan JGY, Chan H-K. Pulmonary drug delivery by powder aerosols. *J Control Release.* 2014;193:228–40.
3. Islam N, Cleary MJ. Developing an efficient and reliable dry powder inhaler for pulmonary drug delivery – a review for multidisciplinary researchers. *Med Eng Phys.* 2012;34(4):409–27.
4. Ógáin ON, Li J, Tajber L, Corrigan OI, Healy AM. Particle engineering of materials for oral inhalation by dry powder inhalers. I—particles of sugar excipients (trehalose and raffinose) for protein delivery. *Int J Pharm.* 2011;405(1):23–35.
5. Jones MD, Price R. The influence of fine excipient particles on the performance of carrier-based dry powder inhalation formulations. *Pharm Res.* 2006;23(8):1665–74.
6. Mangal S, Park H, Nour R, Shetty N, Cavallaro A, Zemlyanov D, et al. Correlations between surface composition and aerosolization of jet-milled dry powder inhaler formulations with pharmaceutical lubricants. *Int J Pharm.* 2019;568:118504.
7. Lucas P, Anderson K, Potter UJ, Staniforth JN. Enhancement of small particle size dry powder aerosol formulations using an ultra low density additive. *Pharm Res.* 1999;16(10):1643–7.
8. El-Sabawi D, Edge S, Price R, Young PM. Continued investigation into the influence of loaded dose on the performance of dry powder inhalers: surface smoothing effects. *Drug Dev Ind Pharm.* 2006;32(10):1135–8.
9. Young PM, Edge S, Traini D, Jones MD, Price R, El-Sabawi D, et al. The influence of dose on the performance of dry powder inhalation systems. *Int J Pharm.* 2005;296(1):26–33.
10. Kinnunen H, Hebbink G, Peters H, Huck D, Makein L, Price R. Extrinsic lactose fines improve dry powder inhaler formulation performance of a cohesive batch of budesonide via agglomerate formation and consequential co-deposition. *Int J Pharm.* 2015;478(1):53–9.
11. Louey MD, Stewart PJ. Particle interactions involved in aerosol dispersion of ternary interactive mixtures. *Pharm Res.* 2002;19(10):1524–31.
12. Shur J, Harris H, Jones MD, Kaerger JS, Price R. The role of fines in the modification of the fluidization and dispersion mechanism within dry powder inhaler formulations. *Pharm Res.* 2008;25(7):1931–40.
13. Dickhoff BJJ, de Boer AH, Lambregts D, Frijlink HW. The effect of carrier surface treatment on drug particle detachment from crystalline carriers in adhesive mixtures for inhalation. *Int J Pharm.* 2006;327(1-2):17–25.
14. Grasmeijer F, Lexmond AJ, van den Noort M, Hagedoorn P, Hickey AJ, Frijlink HW, et al. New mechanisms to explain the

- effects of added lactose fines on the dispersion performance of adhesive mixtures for inhalation. *PLoS One*. 2014;9(1):e87825.
15. Adi H, Larson I, Chiou H, Young P, Traini D, Stewart P. Agglomerate strength and dispersion of salmeterol xinafoate from powder mixtures for inhalation. *Pharm Res* 2007;23(No.11):2556-2565.
 16. Sun Y, Qin L, Liu C, Su J, Zhang X, Yu D, et al. Exploring the influence of drug content on DPI powder properties and potential prediction of pulmonary drug deposition. *Int J Pharm*. 2020;575:119000.
 17. Sun Y, Cui Z, Sun Y, Qin L, Zhang X, Liu Q, et al. Exploring the potential influence of drug charge on downstream deposition behaviour of DPI powders. *Int J Pharm*. 2020;588:119798.
 18. Karner S, Urbanetz NA. Triboelectric characteristics of mannitol based formulations for the application in dry powder inhalers. *Powder Technol*. 2013;235:349–58.
 19. Rudén J, Frenning G, Bramer T, Thalberg K, Alderborn G. Relationships between surface coverage ratio and powder mechanics of binary adhesive mixtures for dry powder inhalers. *Int J Pharm*. 2018;541(1):143–56.
 20. Hertel M, Schwarz E, Kobler M, Hauptstein S, Steckel H, Scherließ R. Powder flow analysis: a simple method to indicate the ideal amount of lactose fines in dry powder inhaler formulations. *Int J Pharm*. 2018;535(1):59–67.
 21. Zellnitz S, Redlinger-Pohn JD, Kappl M, Schroettner H, Urbanetz NA. Preparation and characterization of physically modified glass beads used as model carriers in dry powder inhalers. *Int J Pharm*. 2013;447(1):132–8.
 22. Adi H, Larson I, Chiou H, Young P, Traini D, Stewart P. Role of agglomeration in the dispersion of salmeterol xinafoate from mixtures for inhalation with differing drug to fine lactose ratios. *J Pharm Sci*. 2008;97(8):3140–52.
 23. Zhang X, Zhao Z, Cui Y, Liu F, Huang Z, Huang Y, et al. Effect of powder properties on the aerosolization performance of nanoporous mannitol particles as dry powder inhalation carriers. *Powder Technol*. 2019;358:46–54.
 24. Peng T, Lin S, Niu B, Wang X, Huang Y, Zhang X, et al. Influence of physical properties of carrier on the performance of dry powder inhalers. *Acta Pharm Sin B*. 2016;6(4):308–18.
 25. Cordts E, Steckel H. Capabilities and limitations of using powder rheology and permeability to predict dry powder inhaler performance. *Eur J Pharm Biopharm*. 2012;82(2):417–23.
 26. Lee H-J, Lee H-G, Kwon Y-B, Kim J-Y, Rhee Y-S, Chon J, et al. The role of lactose carrier on the powder behavior and aerodynamic performance of bosentan microparticles for dry powder inhalation. *Eur J Pharm Sci*. 2018;117:279–89.
 27. Faulhammer E, Wahl V, Zellnitz S, Khinast JG, Paudel A. Carrier-based dry powder inhalation: impact of carrier modification on capsule filling processability and in vitro aerodynamic performance. *Int J Pharm*. 2015;491(1):231–42.
 28. Kinnunen H, Hebbink G, Peters H, Shur J, Price R. An investigation into the effect of fine lactose particles on the fluidization behaviour and aerosolization performance of carrier-based dry powder inhaler formulations. *AAPS PharmSciTech*. 2014;15(4):898–909.
 29. Shalash AO, Khalafallah NM, Molokhia AM, Elsayed MMA. The relationship between the permeability and the performance of carrier-based dry powder inhalation mixtures: new insights and practical guidance. *AAPS PharmSciTech*. 2018;19(2):912–22.
 30. Zhou QT, Armstrong B, Larson I, Stewart PJ, Morton DAV. Understanding the influence of powder flowability, fluidization and de-agglomeration characteristics on the aerosolization of pharmaceutical model powders. *Eur J Pharm Sci*. 2010;40(5):412–21.

Publisher's Note Springer Nature remains neutral with regard to jurisdictional claims in published maps and institutional affiliations.